Up and down translocation events and electric double-layer formation inside solid-state nanopores

Mehdi B. Zanjani,[1] Rebecca E. Engelke,[2] Jennifer R. Lukes,[1] Vincent Meunier,[3] and Marija Drndić[2,*]

[1]*Department of Mechanical Engineering and Applied Mechanics, University of Pennsylvania, Philadelphia, Pennsylvania 19104, USA*

[2]*Department of Physics and Astronomy, University of Pennsylvania, Philadelphia, Pennsylvania 19104, USA*

[3]*Department of Physics, Applied Physics, and Astronomy, Rensselaer Polytechnic Institute, Troy, New York 12180, USA*

(Received 3 February 2015; revised manuscript received 3 June 2015; published 19 August 2015)

We present a theoretical study of nanorod translocation events through solid-state nanopores of different sizes which result in positive or negative ion conductance changes. Using theoretical models, we show that positive conductance changes or *up events* happen for nanopore diameters smaller than a transition diameter d_t, and negative conductance changes or *down events* occur for nanopore diameters larger than d_t. We investigate the underlying physics of such translocation phenomena and describe the significance of the electric double-layer effects for nanopores with small diameters. Furthermore, for nanopores with large diameters, it is shown that a geometric model, formulated based on the nanoparticle blockade inside the nanopore, provides a straightforward and reasonably accurate prediction of ion conductance change. Based on this concept, we also implement a method to distinguish and detect nanorods of different sizes by focusing solely on the sign and not the exact value of the conductance change.

DOI: 10.1103/PhysRevE.92.022715 PACS number(s): 87.85.Qr, 87.85.Rs

I. INTRODUCTION

Solid-state nanopores have become increasingly popular tools for characterizing biomolecules [1–9]. Fueled mainly by new potential applications for genomic analysis and DNA sequencing [10,11], nanopore technology has been used to study protein binding and unbinding [12], molecular forces [13,14], DNA-protein interactions [15,16], and even properties of rod-shaped viruses [17]. Nanopores have also found use for studying nanoparticles in applications such as creating and trapping [18,19], or detecting [20,21] and separating [22] nanoparticles, as well as measuring nanoparticle surface charge densities [23]. Nanoparticle translocation causes a change in ion current, or equivalently, in conductance inside nanopores which can be used to characterize the translocating particles. Previous studies have focused on the measurement of such conductance changes [20,23,24] which depend on nanoparticle properties. However, the exact value of the conductance change is hard to describe and is usually presented as an average value with considerable errors [20,23]. It is therefore challenging to characterize nanoparticles based on a correlation between the nanoparticle size or shape and the value of the conductance change. Additionally, a clear theoretical understanding of such systems is not available, which makes it even harder to relate the outputs from experiments to system properties.

Nanoparticle passage through nanopores is usually expected to decrease ion current, similar to the case of typical Coulter counters [25]. In other cases, an increase in conductance has been reported [20,23]. Limited studies on DNA translocation have also mentioned such conductance increases [26,27]. However, the conditions under which the translocation events result in conductance increase or decrease and the implications of such events need further investigation. A clear understanding of such translocation regimes provides valuable insight into the underlying physics and facilitates the definition of predictable and easily distinguishable $(+1)$ and (-1) states that correspond to these positive and negative conductance changes. This leads to new methods for characterizing a wide variety of nanoparticles since detecting an increase or a decrease in conductance is easier and more practical than calculating the exact value of the conductance as a function of system properties.

In this paper, we study nanoparticle translocation events that result either in an increase or in a decrease in ion current. Using theoretical models encompassing fundamental physical principles governing the dynamics of a nanorod-nanopore system, we show that based on the relative size of the nanopore and the nanorod, translocation events with either increasing or decreasing ion currents can happen. We characterize the different regimes observed for nanorod translocation as a function of nanopore diameter and discuss the conditions under which using a straightforward model based on the geometric blockade is sufficiently accurate to describe translocation events. We also study the translocation of nanorods with different sizes and demonstrate a method to characterize and distinguish nanorods based solely on detecting translocation events with positive or negative ion current changes.

II. THEORETICAL MODEL

We begin our study by considering a nanorod translocating through nanopores of different diameters as shown schematically in Fig. 1. In this setup, nanopores are positioned in a thin membrane to divide two chambers of ionic solutions such that the pores are the only path for ion transport between the chambers. When a potential is applied across the nanopores, a steady ionic current is observed. The open-pore current corresponds to this steady current in the absence of nanorods. As the nanorods, which carry a positive surface charge, translocate through the nanopores, one by one, their presence results in a change in the current density inside the nanopores. This current change, or the equivalent conductance change, is a key, experimentally available, quantity for characterizing translocation events. We use the terminology *up event* when an increase in the ionic

*drndic@physics.upenn.edu

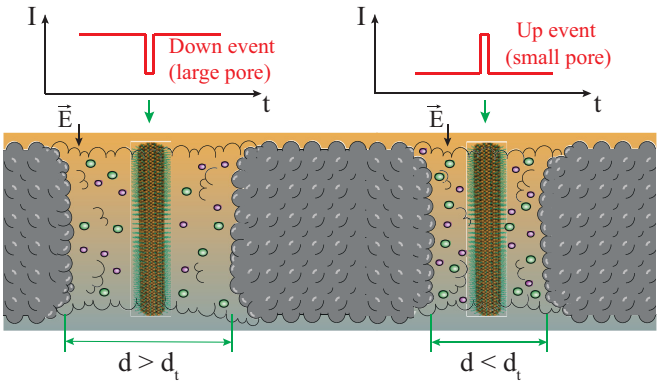

FIG. 1. (Color online) Schematic of nanorod translocation through two nanopores of different diameters. The nanopore membrane is shown in gray. The nanorod is shown in orange in the middle of the pore. Cation and anions are shown by the small and large spheres.

current is observed. Similarly, a *down event* refers to a decrease in the ionic current. Here we investigate the conditions under which such events will happen. We use a theoretical model to analyze the nanopore-nanorod system and study these up and down events. In the systems we study here, the nanorod surface is covered by cetyltrimethylammonium bromide ligands [28]. The nanopore walls are also covered with surface functionalizing groups [23,28]. We consider an average 1.5 nm increase for nanorod diameter and a corresponding 1.5 nm decrease in the nanorod diameter to build the suitable geometry that takes into account the presence of the ligands.

To study up and down events, we first need to calculate the open-pore conductance G_0. In the absence of the translocating nanorod, the total current is a combination of the contributions of the bulk concentration of ions and the positive ions shielding the negatively charged nanopore walls [26,29]. Therefore, G_0 is calculated based on

$$G_0 = \frac{\pi d_{\text{pore}}^2}{4L_{\text{pore}}}(\mu_{K_+} + \mu_{Cl_-})Fc_0 + \frac{\pi d_{\text{pore}}}{L_{\text{pore}}}\mu_{K_+}\sigma_{\text{pore}}. \qquad (1)$$

Here F is the Faraday constant, μ_{K_+} and μ_{Cl_-} are the mobility of the cations and anions, c_0 is the bulk concentration of ions inside the nanopore, and σ_{pore} is the surface charge density of the nanopore. L_{pore} and d_{pore} represent the length and diameter of the nanopore. For the system we study here, $L_{\text{pore}} = 42$ nm, $\sigma_{\text{pore}} = -2.3\times10^{-2}$ C/m^2, $\mu_{K_+} = 6.10\times10^{-8}$, $\mu_{Cl_-} = 6.36\times10^{-8}$ m^2 V^{-1} s^{-1}, and $c_0 = 100$ mM [27]. The nanopore diameter d_{pore} is the variable parameter in the model and is considered to be between 17 and 28 nm.

To calculate the conductance change due to the translocation of a nanorod, we note that the nanorod blocks a portion of the ionic current due to the volume it occupies inside the pore. This blockade effect yields a conductance reduction (i.e., $\Delta G < 0$). On the other hand, since the nanorod walls carry a positive charge, the anions inside the electrolyte solution that surround the nanorod follow the movement of the nanorod and therefore induce an increase in anionic current. By considering the superposition of these two opposing effects, we can now calculate the total change in conductance due to nanorod translocation as

$$\Delta G = -\frac{\pi d_{\text{rod}}^2}{4L_{\text{pore}}}(\mu_{K_+} + \mu_{Cl_-})Fc_0 + \frac{\mu_{Cl_-}}{L_{\text{pore}}}\lambda_q, \qquad (2)$$

where d_{rod} is the nanorod diameter. For the first term of Eq. (2), the nanorod occupies a region inside the nanopore where ion concentrations are equal to the bulk concentration c_0 in an open-pore system in the absence of the nanorod. In the second term of Eq. (2), λ_q denotes the effective charge per unit length of the counterions screening the nanorod wall, which introduces the positive contribution to the total conductance change [26]. The value of λ_q is dependent on the distribution of ion concentration in the space between the nanopore and the nanorod walls. Since both the nanopore and the nanorod walls are charged, electric double layers are formed next to each wall due to the presence of shielding counterions. When the nanopore and nanorod walls are far away from each other, i.e., in larger nanopores, the shielding counterions of the nanorod are not influenced by the nanopore walls. In this case, λ_q is essentially equal to the charge per unit length of the nanorod as the shielding counterions are just affected by the surface charge of the nanorod. However, as the nanorod and nanopore walls become closer to each other, i.e., in smaller nanopores, the double layers start overlapping and influencing each other, thereby affecting λ_q. If the nanopore wall is close to the nanorod wall, it will magnify the effect of the negative charges shielding the nanorod wall since the nanopore wall is negatively charged and will push the negative ions away from itself and towards the nanorod wall. This will result in an increase in λ_q as the nanorod and nanopore walls get closer to each other.

Variations in λ_q as a function of the relative nanorod-nanopore size can be alternatively explained by studying the effective force acting on the nanorod. This is essentially the driving force for nanorod translocation which in turn induces a positive conductance change by displacing the shielding counterions around the nanorod. The total effective force F_{eff}, acting on translocating particles is a combination of the bare electric force and electroosmotic forces [13]. This force can be represented by [13,30] $F_{\text{eff}} = \lambda_{\text{eff}}\Delta\phi$, where $\Delta\phi$ is the applied potential across the nanopore and λ_{eff} represents the effective charge per unit length, similar to λ_q in our model. Since in our model λ_q decreases as nanopore diameter increases, it suggests that the effective force decreases as the nanopore size increases. This observation is in agreement with previous theoretical and experimental studies of the effective force acting on rod-shaped DNA molecules translocating through solid-state nanopores [13,31].

Next, in order to define the two regimes discussed above more rigorously, we introduce a quantity $d_{\text{separation}}$ which represents the difference between the pore and the rod diameters beyond which electric double layers do not overlap. The value of $d_{\text{separation}}$ can be calculated based on the thickness of the double layers next to the nanorod and nanopore walls. For this purpose, we calculate the cation and anion concentrations c_{K_+} and c_{Cl_-} from the numerical solution of the Navier-Stokes and Poisson-Nernst-Planck equations [29,30,32]. The resulting concentration profiles are shown in Fig. 2. By considering the ion concentration profile for larger nanopores, such as the system with a 28 nm nanopore shown in Fig. 2(b), we find that double layers next to the nanorod and the nanopore are

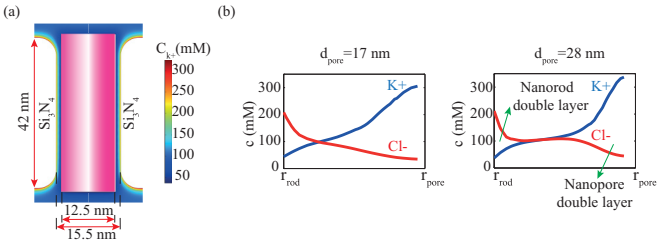

FIG. 2. (Color online) (a) Cation concentration inside the nanopore in the presence of a translocating nanorod. (b) Ion concentration in the space between the nanorod and the nanopore for a smaller 17 nm and a larger 28 nm nanopore. $r_{\rm rod}$ and $r_{\rm pore}$ represent the nanorod and nanopore radii.

approximately 1.5 and 2 nm thick, respectively. Considering the 1.5 nm combined length of the surface functionalizing groups attached to the outside surface of the nanorod and the inside surface of the nanopore, we estimate a value of $r_{\rm separation} \sim 5$ or $d_{\rm separation} \sim 10$ nm. Thus, with $d_{\rm separation}$ determined, if $d_{\rm pore} - d_{\rm rod} > d_{\rm separation}$, λ_q is constant and can be calculated as the charge per unit length of the nanorod, i.e., $\lambda_{q0} = \pi d_{\rm rod}\sigma_{\rm rod}$ where $\sigma_{\rm rod} = 1.8\times10^{-2}$ C/m^2 is the surface charge density of the nanorod [23]. When $d_{\rm pore} - d_{\rm rod} < d_{\rm separation}$, λ_q will increase. Based on experimental measurements [23], for a 11 nm diameter nanorod inside a $d_{\rm pore1} = 19$ nm nanopore, $\Delta G/G_0$ around 20% is observed which can be equivalently obtained using $\lambda_{q1} = 3.2$ nC/m with Eqs. (1) and (2). With λ_{q0} and λ_{q1} in hand, we use a simple linear curve fit to calculate the values of λ_q for nanopore diameters that satisfy the condition $d_{\rm pore} - d_{\rm rod} < d_{\rm separation}$.

III. RESULTS AND DISCUSSION

After calculating λ_q, we can use Eqs. (1) and (2) to calculate G_0 and ΔG for different nanopore diameters. Figure 3(a) shows a schematic of the the nanopore-nanorod system. The resulting relative conductance change $\Delta G/G_0$ is shown in Fig. 3(b) for different nanopore diameters. For small nanopore diameters, positive ΔG, or up events, are observed whereas for large nanopore diameters ΔG is negative, corresponding to a down event. A similar trend is observed from the few available experimental values [23], which have not been explained quantitatively before and are in good agreement with our theoretical model. More specifically, for the 11 nm nanorods, up events happen when nanopore diameter is smaller than $d_t \simeq 19.9$ nm which we call the *transition diameter*. For nanopore diameters larger than the transition diameter, down events occur. Therefore, d_t presents a measure for detecting (+1) and (−1) states that are defined simply based on the sign of $\Delta G/G_0$.

Looking at the simulation results for $\Delta G/G_0$ versus the nanopore diameter, we observe two different regions in Fig. 3(b). The red curve (surrounded by the shaded area) describes a simple model based on the geometric blockade of the nanorod inside the nanopore that can provide a fairly accurate description. We call this model the *geometric model* which expresses ΔG with respect to the amount of space occupied by the nanorod inside the nanopore. Since the nanopore and the nanorod represent cylindrical geometries, the ionic current change relative to the open-pore current will be proportional to the reduction in cross-sectional surface area of the nanopore in the presence of the nanorod, i.e., $\Delta G/G_0 = -\frac{d_{\rm nr}^2}{d_{\rm pore}^2}$ where $d_{\rm nr}$ represents the effective diameter of the nanorod. This geometric model provides a rather simple explanation of the ion conductance change due to nanorod translocation; the negative sign implies a reduction in the ion current. Comparing the theoretical model results to the geometric model reveals that this model is only valid for down events when the nanopore diameter is larger than a specific value denoted by d_g. For the system discussed in Fig. 3(a), we have $d_g \simeq 21$ nm. The red curve in Fig. 3(b) represents the geometric model $-\frac{d_{\rm nr}^2}{d_{\rm pore}^2}$ with an effective nanorod diameter of $d_{\rm nr}^{\rm eff} = 11.25$ nm. The bounding shaded area is described by the same model with $d_{\rm nr}$ limits corresponding to $d_{\rm nr}^{\rm eff} \pm 6.7\%$. This result shows it is possible to use a straightforward geometric model to describe the ion conductance change similar to typical Coulter counters, however, this approximation is only valid for nanopore diameters larger than d_g. Additionally,

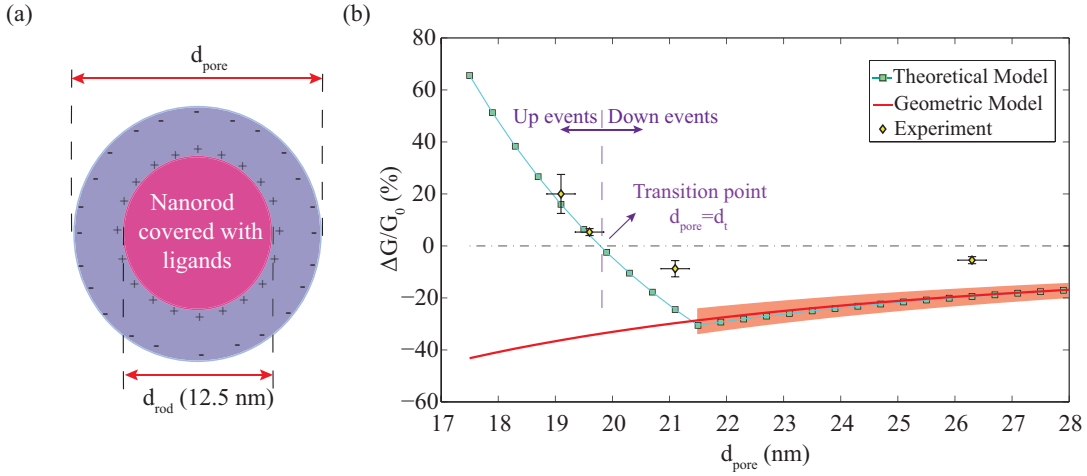

FIG. 3. (Color online) (a) Cross-sectional view of the nanopore-nanorod system. The nanorod wall is covered with ligands and carries a positive charge, whereas the nanopore wall carries a negative charge. (b) $\Delta G/G_0$(%) versus the nanopore diameter $d_{\rm pore}$, obtained from the theoretical model in comparison to experimental data. The red curve (surrounded by the shaded area) represents the simple geometric model.

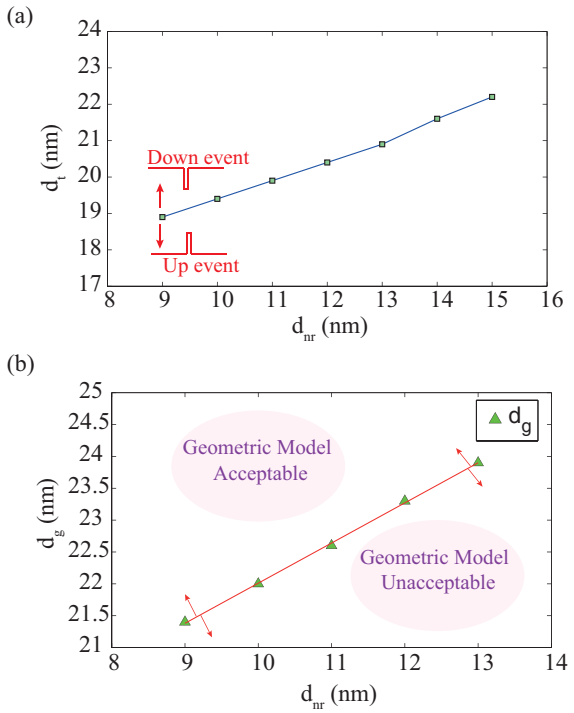

FIG. 4. (Color online) (a) d_t as a function of nanorod diameter. (b) d_g values for nanorods of different diameters.

we also calculated the Dukhin length [33] l_{Du} to study the effect of surface conductance. For the system we consider here, the Dukhin length is about 0.9 nm, approximated based on $l_{\mathrm{Du}} = (|\sigma_{\mathrm{rod}}|/e)/(2c_0)$ where σ_{rod} is the nanorod surface charge density and e is the electron charge [33]. When the nanopore wall and the nanorod walls are close to each other, the Dukhin length is relatively large, thus the surface conductivity effect by the rod becomes significant and contributes to λ_{eff}. To summarize, the combination of the effects of Debye layer, Dukhin layer, and geometrical blockade is responsible for the conductance change with the first two effects reflected in λ_{eff}. It is also worth mentioning that as F_{eff} is partially determined by electroosmotic force, the electroosmotic effect is another source that influences the total conductance change [34]. Furthermore, we define a dimensionless quantity $d^* = (d_{\mathrm{pore}} - d_{\mathrm{rod}})/(l_{\mathrm{De}} + l_{\mathrm{Du}})$ based on the nanopore and nanorod diameters and the Debye (l_{De}) and Dukhin (l_{Du}) lengths. Based on the calculation of $d_{\mathrm{separation}}$ and the double-layer and Dukhin lengths in the previous discussion, the geometric model will be valid for $d^* > 2.3$. This provides a simpler measure based on a dimensionless quantity defined by the physical parameters of the system.

Next, revisiting Fig. 3(b), we look at the up and down events and the validity of the geometric model in more detail. In Fig. 4(a), we studied the transition between up and down events for nanorods of different diameters by calculating d_t from the theoretical model. For each nanoparticle diameter the value of d_t determines the nanopore diameter above which down events are observed and below which up events are observed. Figure 4(a) shows the resulting d_t values for nanorods with diameters in the 9–15 nm range. This plot provides different choices of nanopore diameter that result in up events for nanorods of a given size and down events for nanorods of another size. For example, if we consider a 10 and a 14 nm nanorod translocating through a 20 nm nanopore, up events are observed for the 14 nm nanorod and down events are observed for the 10 nm nanorod. Such combinations of (+1) and (−1) states provide a powerful tool to detect and distinguish nanorods of different sizes based solely on the sign of the current change. In particular, if we consider an electrolyte solution that contains two different sizes of nanorods, provided that appropriate conditions based on Fig. 4(a) are satisfied, applying an external voltage will result in the observation of both up and down translocation events. Each (+1) state, i.e., positive ion current change, represents the translocation of the larger nanorod, and each (−1) state, i.e., negative ion current change, represents the translocation of a smaller nanorod. Therefore, the plot in Fig. 4(a) provides a blueprint for designing nanoparticle detection or counting devices that can distinguish between nanoparticles of different sizes. Also, the fact that this design will only be based on positive or negative current change observations and not on the exact value of the current change increases the effectiveness of this method since comparing exact numerical values needs extra computational and experimental efforts and is often subjected to different possible errors.

We can also determine the conditions for the validity of the geometric model for nanorods of different sizes by calculating the corresponding d_g. Figure 4(b) shows the value of d_g calculated for nanorods of different diameters. This figure provides valuable knowledge about using the straightforward geometric model to get an accurate estimate of the ion conductance change. For each specific nanorod diameter, the geometric model is only valid for nanopore diameters larger than the corresponding d_g. By considering the curve formed by connecting the points in Fig. 4(b), we can determine whether the geometric model is valid or not, given both the nanorod and the nanopore diameters. If the corresponding point (d_{nr},d_{pore}) lies above the curve in Fig. 4(b), using the geometric model is reasonable, whereas if this point lies below the curve, the geometric model is prone to significant errors. It is also worth mentioning that the farther above the (d_{nr},d_{pore}) point from the curve is, the more accurate the geometric model will be.

IV. CONCLUSIONS

In conclusion, we have demonstrated different regimes in the translocation of nanorods through solid-state nanopores and showed that up and down events can be observed independently based on the relative nanoparticle and nanopore sizes. Up events take place in systems with smaller nanopore diameters, whereas for larger nanopore diameters, down events occur. We also demonstrated how (+1) and (−1) states can be helpful to implement a simple way for distinguishing nanorods of different sizes with a simple algorithm based on the observation of positive and negative changes in the conductance. This general approach might pave the way for using solid-state nanopores as fast electronic sensors to detect and characterize a wide variety of nanoparticles with different sizes and shapes.

ACKNOWLEDGMENT

This work was supported by the NSF MRSEC Grant No. DMR-1120901.

[1] S. Howorka and Z. Siwy, Chem. Soc. Rev. **38**, 2360 (2009).
[2] B. M. Venkatesan and R. Bashir, Nat. Nanotechnol. **6**, 615 (2011).
[3] F. Haque, J. Li, H.-C. Wu, X.-J. Liang, and P. Guo, Nano Today **8**, 56 (2013).
[4] D. Deamer and M. Akeson, Trends Biotechnol. **18**, 147 (2000).
[5] D. Deamer and D. Branton, Acc. Chem. Res. **35**, 817 (2002).
[6] K. Healy, B. Schiedt, and A. P. Morrison, Nanomedicine **2**, 875 (2007).
[7] D. Branton, D. W. Deamer, A. Marziali, H. Bayley, S. A. Benner, T. Butler, M. Di Ventra, S. Garaj, A. Hibbs, X. Huang, S. B. Jovanovich, P. S. Krstic, S. Lindsay, X. S. Ling, C. H. Mastrangelo, A. Meller, J. S. Oliver, Y. V. Pershin, J. M. Ramsey, R. Riehn, G. V. Soni, V. Tabard-Cossa, M. Wanunu, M. Wiggin, and J. A. Schloss, Nat. Biotechnol. **26**, 1146 (2008).
[8] C. Dekker, Nat. Nanotechnol. **2**, 209 (2007).
[9] J. J. Kasianowicz, J. W. F. Robertson, E. R. Chan, J. E. Reiner, and V. M. Stanford, Annu. Rev. Anal. Chem. **1**, 737 (2008).
[10] M. Zwolak and M. D. Ventra, Rev. Mod. Phys. **80**, 141 (2008).
[11] M. Wanunu, Phys. Life Rev. **9**, 125 (2012).
[12] K. J. Freedman, M. Jürgens, A. Prabhu, C. W. Ahn, P. Jemth, J. B. Edel, and M. J. Kim, Anal. Chem. **83**, 5137 (2011).
[13] U. F. Keyser, B. N. Koeleman, S. van Dorp, D. Krapf, R. M. M. Smeets, S. G. Lemay, N. H. Dekker, and C. Dekker, Nat. Phys. **2**, 473 (2006).
[14] O. K. Dudko, J. Mathe, A. Szabo, A. Meller, and G. Hummer, Biophys. J. **92**, 4188 (2007).
[15] A. R. Hall, S. van Dorp, S. G. Lemay, and C. Dekker, Nano Lett. **9**, 4441 (2009).
[16] S. W. Kowalczyk, A. R. Hall, and C. Dekker, Nano Lett. **10**, 324 (2010).
[17] A. McMullen, H. W. de Hann, J. X. Tang, and D. Stein, Nat. Commun. **5**, 1 (2014).
[18] K. Venta, M. Wanunu, and M. Drndić, Nano Lett. **13**, 423 (2013).
[19] R. Sharabani, S. Reuveni, G. Noy, E. Shapira, S. Sadeh, and Y. Selzer, Nano Lett. **8**, 1169 (2008).
[20] G. Goyal, K. J. Freedman, and M. J. Kim, Anal. Chem. **85**, 8180 (2013).
[21] E. Campos, C. E. McVey, R. P. Carney, F. Stellacci, Y. Astier, and J. Yates, Anal. Chem. **85**, 10149 (2013).
[22] A. S. Prabhu, T. Z. N. Jubery, K. J. Freedman, R. Mulero, P. Dutta, and M. J. Kim, J. Phys.: Condens. Matter **22**, 454107 (2010).
[23] K. E. Venta, M. B. Zanjani, X. Ye, G. Danda, C. B. Murray, J. R. Lukes, and M. Drndić, Nano Lett. **14**, 5358 (2014).
[24] H. Wu, H. Liu, S. Tan, J. Yu, W. Zhao, L. Wang, and Q. Liu, J. Phys. Chem. C **118**, 26825 (2014).
[25] W. H. Coulter, U.S. Patent No. 2,656,508 (20 October 1953).
[26] R. Smeets, U. Keyser, D. Krapf, M. Wu, N. Dekker, and C. Dekker, Nano Lett. **6**, 89 (2006).
[27] D. M. Vlassarev and J. A. Golovchenko, Biophys. J. **103**, 352 (2012).
[28] X. Ye, L. Jin, H. Caglayan, J. Chen, G. Xing, C. Zheng, V. Doan-Nguyen, Y. Kang, N. Engheta, C. R. Kagan, and C. B. Murray, ACS Nano **6**, 2804 (2012).
[29] J. C. Berg, *An Introduction to Interfaces and Colloids* (World Scientific, Singapore, 2010).
[30] B. Lu, D. P. Hoogerheide, Q. Zhao, and D. Yu, Phys. Rev. E **86**, 011921 (2012).
[31] S. van Dorp, U. F. Keyser, N. H. Dekker, C. Dekker, and S. G. Lemay, Nat. Phys. **5**, 347 (2009).
[32] G. K. Batchelor, *An Introduction to Fluid Dynamics* (Cambridge University Press, Cambridge, UK, 2000).
[33] C. Lee, L. Joly, A. Siria, A.-L. Biance, R. Fulcrand, and L. Bocquet, Nano Lett. **12**, 4037 (2012).
[34] L. Bocquet and E. Charlaix, Chem. Soc. Rev. **39**, 1073 (2010).